American Mineralogist, Volume 63, pages 1252–1259, 1978

Thermal changes in monoclinic tridymite

AKIHIKO NUKUI, HIROMOTO NAKAZAWA

National Institute for Researches in Inorganic Materials
Kurakake, Sakura-mura, Niihari-gun, Ibaraki, 300–31 Japan

AND MASARU AKAO

Tokyo Institute of Technology
Ookayama, Meguro-ku, Tokyo, 152 Japan

Abstract

Thermal changes in tridymite were examined at high temperatures by X-ray single-crystal and optical methods, using a hydrothermally-synthesized crystal of monoclinic modification. Five phases were confirmed on heating and cooling. They were MC, OP, OS, OC, and HP phases, in the temperature ranges from room temperature to 110°, 110°–150°, 150°–190°, 190°–380°, and above 380°C respectively: MC, monoclinic Cc, a = 18.49, b = 4.991, c = 25.83A, β = 117.75°; OP, orthorhombic $P2_12_12_1$, a = 26.65, b = 5.02, c = 8.15A; OS, metrically orthorhombic with a non-integral superstructure, a = variable from 95 to 65, b = 5.02, c = 8.18A; OC, orthorhombic $C222_1$, a = 8.73, b = 5.04, c = 8.28A; HP, hexagonal $P6_3/mmc$, a = 5.05, c = 8.28A.

Introduction

Tridymite has several modifications stable at room temperatures. Some low-temperature forms have been reported by Buerger and Lukesh (1942) and Hill and Roy (1958), and the crystal structures of two of them have been determined by Kato and Nukui (1976) (independently by Dollase and Baur, 1976) and Konnert and Appleman (1975) respectively. Two modifications at higher temperatures have been proposed. The crystal structure of one of them has been determined by Dollase (1968) at 220°C. The other structure above that temperature has been proposed by Gibbs (1927).

The transitions of tridymite have been extensively studied since Fenner (1913) found two transitions at 117° and 163°C. Sosman (1965) has summarized the data of thermal changes in tridymites reported by many other investigators and proposed a list of thermal phase boundaries of tridymite consistent with these data. However, the crystallographic relationships of each modification at room and at higher temperatures were not clear, because the previous studies were mainly based on differential thermal, dilatometric, or X-ray powder-diffraction analyses. From the crystallographic point of view, only a few reports presented data taken at high temperatures (see Fig. 9).

In the present study, a hydrothermally-synthesized low-tridymite (monoclinic modification), which was well-characterized, was examined systematically at increasing and decreasing temperatures by means of X-ray single-crystal diffraction and polarization-microscopic methods. The phases at higher temperatures, including some new modifications, are described in the following sections.

Experimental

Crystals of tridymite were synthesized under hydrothermal conditions from a high-purity synthetic fused silica. The silica glass, a minor amount of sodium carbonate, and pure water were sealed in a platinum capsule. The capsule was placed in a pressure vessel and kept at 500 kg/cm² and 1100°C for 14 days.

The crystals produced were colorless transparent hexagonal or wedge-shaped platelets with maximum size of 2.0 × 1.0mm. Impurities in the products were examined by chemical and emission spectroscopic analyses, and the impurities such as B, Mg, Fe, Al, Na, and hydroxyl do not exceed about 50ppm in

0003–004X/78/1112–1252$02.00

weight. Many crystals showed uniform extinction under crossed nicols when observed normal to the platelet (*c* axis of the hexagonal high form), thus they seem to be a single domain.

These crystals were examined by the X-ray precession and Weissenberg methods at room and at high temperatures. For the precession method, the crystal was supported by a silica-glass capillary and was heated by an alumina-coated platinum furnace. For the Weissenberg method, the crystal was attached with alumina cement to the top of a silica-glass capillary and was heated by a platinum cylindrical heater. The temperatures were controlled throughout the experiments in the range of ±2°C at about 500°C for both methods. Some crystals were also subjected to heating experiments under the polarization microscope with the platinum cylindrical heater.

Results

Five phases were observed to be stable below 450°C. With increasing temperature, detectable changes were found at 110°, 150°, 190°, and 380°C. The phases observed in the ranges from room temperature to 110°, 110°–150°, 150°–190°, 190°–380°, and above 380°C are named MC, OP, OS, OC, and HP phases, based on their respective symmetries. The transition between HP and OC phases is reversible. The transitions from OC to OS phases and from OS to OP phases showed slight hysteresis, and from OP to MC phases relatively large hysteresis. The relations between these phases were also confirmed by polarization microscopic observation. Figures 1a–1h show photomicrographs of a tridymite crystal which were taken stepwise at temperatures between room temperature and 450°C. Detailed crystallographic relations among them are as follows.

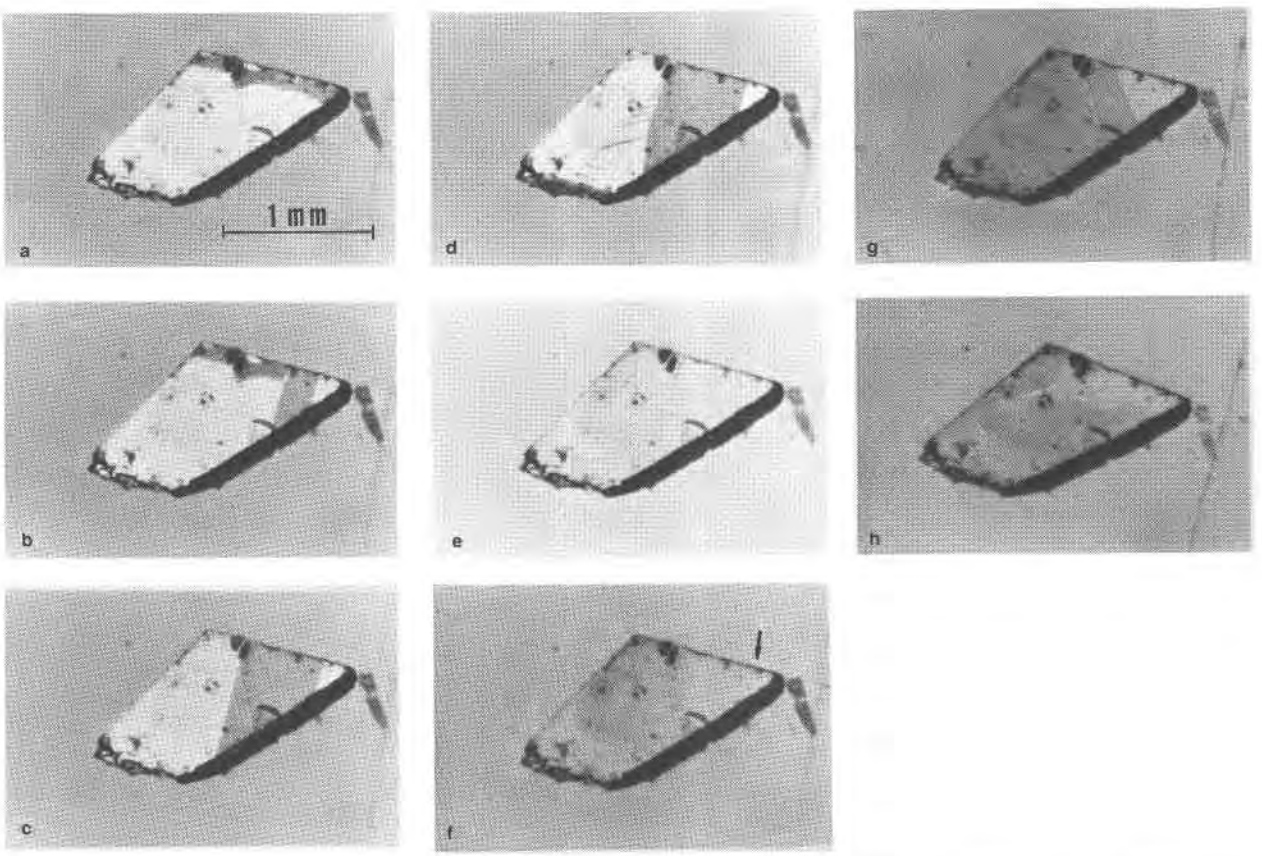

Fig. 1. Photomicrographs under polarized light of a tridymite crystal, taken stepwise in the temperature range between room temperature and 450°C. (a) at room temperature (MC phase). (b) at 110°C, the beginning of transition from MC to OP phases. (c) at above 110°C, stable domains after the transition (OP phase). (d) at 150°C, the beginning of transition from OP to OS phases. (e) at above 150°C, apparently a single crystal after the transition (OS phase). (f) at 190°C, the beginning of transition from OS to OC phases. (g) at above 190°C, growth of domain and forming of polysynthetic lamellae (OC phase). (h) at above 380°C (HP phase).

MC phase

The tridymite crystals are monoclinic at room temperature with space group Cc; $a = 18.49$, $b = 4.991$, $c = 25.83$A, $\beta = 117.75°$, and $Z = 48$. The axial relations between the MC phase and HP phase are

$$\begin{Bmatrix} a_{MC} \\ b_{MC} \\ c_{MC} \end{Bmatrix} = \begin{Bmatrix} 2 & 1 & 2 \\ 0 & 1 & 0 \\ \bar{6} & \bar{3} & 0 \end{Bmatrix} \cdot \begin{Bmatrix} a_{HP} \\ b_{HP} \\ c_{HP} \end{Bmatrix}$$

The crystals are usually twinned by 180° rotation about $[301]_{MC}$ (c_{HP}). The crystal structure of this phase has been determined by Kato and Nukui (1976) and Dollase and Baur (1976). Figure 2 shows an $\bar{h}k3h$ precession photograph of this phase at room temperature. Similar diffraction patterns with monoclinic symmetry were observed at all temperatures below 110°C, and there were no detectable changes, including the intensity distribution.

OP phase

An $hk0$ precession photograph of the OP phase at 110°C is reproduced in Figure 3. The $hk0$ net of the OP phase is schematically illustrated for convenience in understanding the twinning relations (Fig. 4). Though this diffraction pattern seems to be complex because of six- or three-fold twinning about c_{OP} (c_{HP}), the systematic absences are $h \neq 2n$ for $h00$, $k \neq 2n$ for $0k0$ and $l \neq 2n$ for $00l$. The true unit cell is therefore orthorhombic in space group $P2_12_12_1$, with $a = 26.65$, $b = 5.02$, $c = 8.15$A (indicated as ABCD in Fig. 4). The mutual relationships between $(a^*_{MC}, b^*_{MC}, c^*_{MC})$ and $(a^*_{OP}, b^*_{OP}, c^*_{OP})$ are as follows,

$$a^*_{MC} \simeq c^*_{OP}$$
$$b^*_{MC} \simeq b^*_{OP}$$
$$c^*_{MC} \simeq -a^*_{OP} + c^*_{OP}$$

The axial relationships of real lattices among MC, OP, and HP phases are

$$\begin{matrix} a_{OP} \\ b_{OP} \\ c_{OP} \end{matrix} = \begin{Bmatrix} 0 & 0 & \bar{1} \\ 0 & 1 & 0 \\ 1/2 & 0 & 1/6 \end{Bmatrix} \cdot \begin{matrix} a_{MC} \\ b_{MC} \\ c_{MC} \end{matrix}$$

$$\begin{matrix} a_{OP} \\ b_{OP} \\ c_{OP} \end{matrix} = \begin{Bmatrix} 6 & 3 & 0 \\ 0 & 1 & 0 \\ 0 & 0 & 1 \end{Bmatrix} \cdot \begin{matrix} a_{HP} \\ b_{HP} \\ c_{HP} \end{matrix}$$

Here we can choose an apparent cell where the presence of twinning is neglected, as is indicated by EFGH in Figure 4. This apparent cell is orthorhombic with $a' = 53.30$, $b' = 30.12$, $c' = 48.90$A, and the main reflections reveal a $C222_1$ space group. A modification reported by Götz (1962) corresponds to this apparent cell, and thus it might be a quenched form from the temperature range of the OP phase.

With decreasing temperature, transition from OP to MC phases was at about 75°C. In most cases, the structure after this transition was the same as the starting structure, but tended to have six-fold twinning.

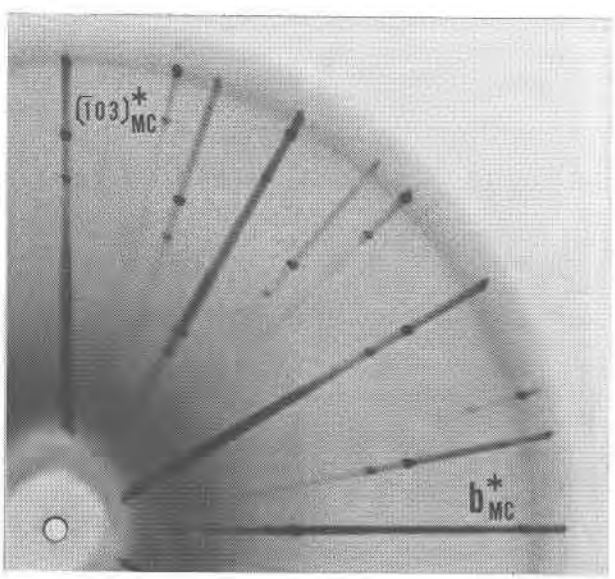

Fig. 2. Precession photograph of $\bar{h}k3h$ net (reciprocal plane normal to a^*_{MC}) of the MC phase taken at room temperature.

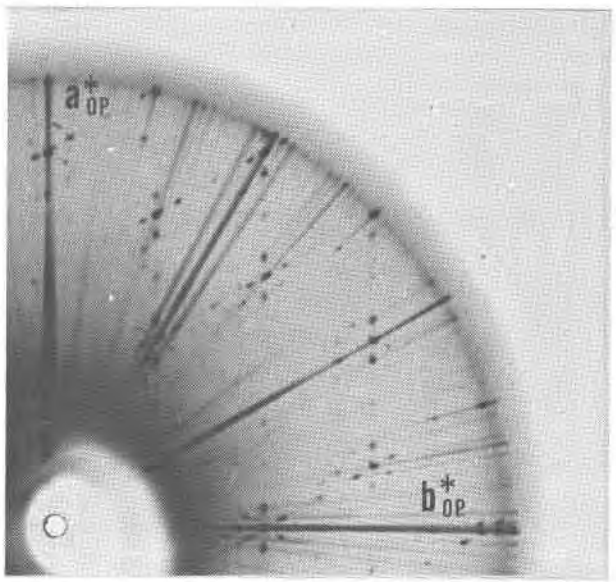

Fig. 3. Photograph of the $hk0$ net of the OP phase at 110°C.

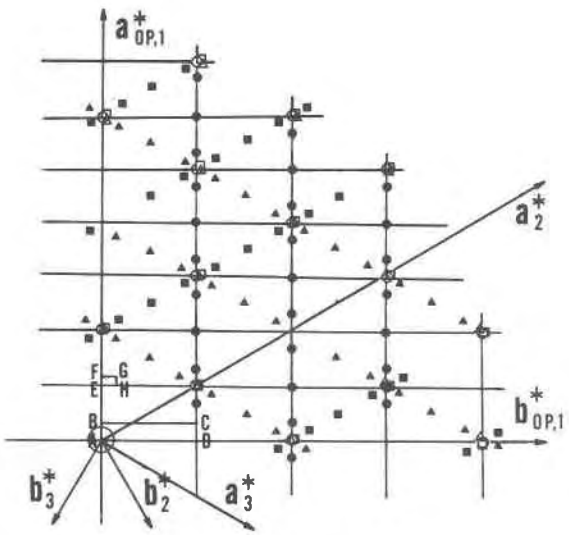

Fig. 4. Schematically-illustrated *hk*0 net of the OP phase observed. For convenience the reflections from different twin individuals are indicated differently by circles, triangles, and squares. Open symbols reveal main reflections. The rectangle ABCD indicates the true unit cell of the OP phase, and EFGH the apparent cell (see text), where their c^* axes are normal to and downwise to the paper.

Under the polarizing microscope at room temperature, most parts of the crystal showed uniform extinction in the direction normal to the platelet corresponding to $[301]_{MC}$, occasionally having small domains bounded with curved lines (Fig. 1a). On heating, different forms of domains, relative to the original, start to form rapidly at 110°C (Fig. 1b), and then immediately settle down to several domains (two or three in most cases) which are bounded by straight lines and oriented at 60° to each other (Fig. 1c). These domains keep their orientation and boundaries up to about 150°C. The hysteresis of transition from OP to MC phases is also observed optically. With decreasing temperature, below 75°C, complicated domain texture bounded by curved lines appeared in the crystal. This domain texture may correspond to twinning.

OS phase

With increasing temperature, the second change was observed at about 150°C. Figures 5a and 5b show photographs of the *hk*0 nets of the OS phases at 150° and 180°C respectively. The photographs indicate additional satellite reflections in the a^*_{OS} direction, which corresponds to $[210]_{HP}$. Six-fold twinning is also seen (Fig. 5). The strong reflections reveal a $C222_1$ space group. The supercell is metrically orthorhombic. The spacing of these satellite reflections indicated that the period varies from 95A at 150°C to 65A at about 190°C. The dimensions are, therefore, a = 95–65, b = 5.02, c = 8.18A. The period of the satellites may vary continuously in a way similar to the long period observed in pyrrhotite (Nakazawa and Morimoto, 1971) and feldspar (Megaw, 1960; Kitamura and Morimoto, 1975). A similar phenomenon has briefly been mentioned by Dollase (1968) for a different temperature range. Diffuse streaks newly appear in the direction of the long period, which may indicate stacking faults or some other crystal imperfections (Fig. 5). In the vicinity of 190°C, the satellite reflections change to diffuse streaks in the same direction.

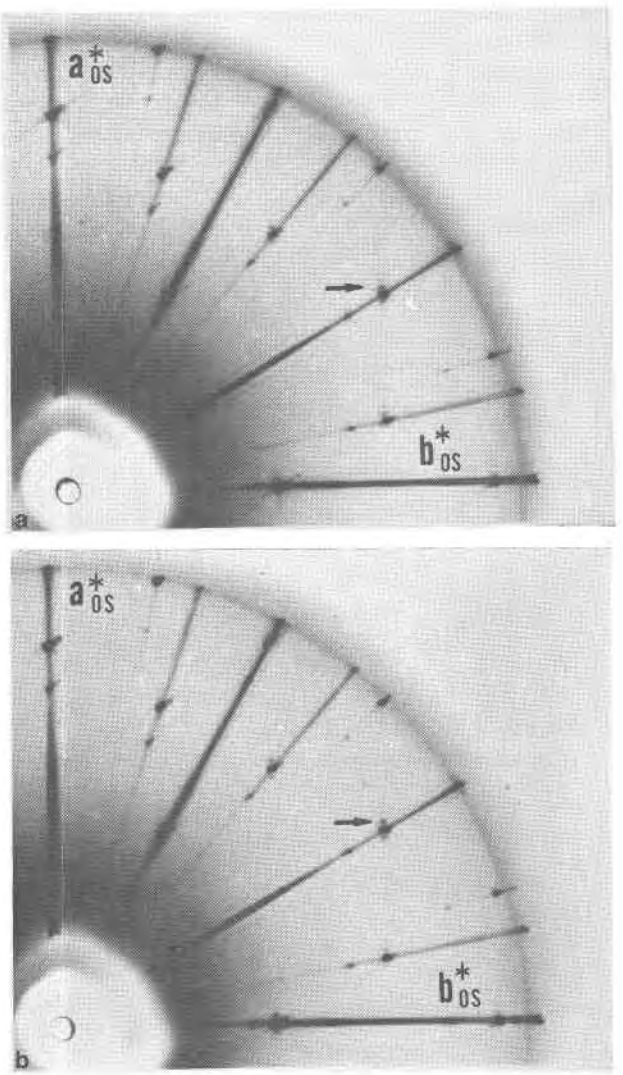

Fig. 5. Photographs of the *hk*0 net of the OS phase: (a) at 150°C; (b) at 180°C.

Under the microscope, it was observed that the OS phase was grown as many streak-like domains close to but above the transition temperature (Fig. 1d), and spread throughout the crystal with increasing temperature, where the crystal seemed to be a single domain (Fig. 1e).

OC phase

Figure 6 shows a photograph of the *hk*0 net of the OC phase at 260°C, in which main reflections are accompanied by faint diffuse streaks along the a^*_{OC} direction. Reflections, except the diffuse streaks, indicate that this phase is orthorhombic, $C222_1$, with $a = 8.73$, $b = 5.04$, $c = 8.28$A, since the systematic absences are $h + k \neq 2n$ for *hkl* and $l \neq 2n$ for 00*l*. This phase is identical with that described by Dollase (1968), if the diffuse streaks are neglected.

Under the optical microscope, the transition from OS to OC phases starts at a corner of the crystal (Fig. 1f) at about 200°C. The domain formed becomes slightly larger, and, simultaneously, polysynthetic lamellae are observed parallel to or oriented at 60° or 120° to crystal edges. Then polysynthetic lamellae gradually spread throughout the crystal (Fig. 1g) with increasing temperature up to about 380°C. Above about 380°C, polysynthetic lamellae become vague and the domain located at the corner of the crystal below the transition temperature vanishes.

HP phase

The fourth change was observed at the vicinity of 380°C. The photograph of the *hk*0 net taken at 380°C is shown in Figure 7. The photograph indicates that the HP phase belongs to Laue group 6/*mmm*. The HP phase is in space group $P6_3/mmc$, since the systematic absence is $l \neq 2n$ for $hh2\bar{h}l$ only. Cell dimensions of the HP phase are $a = 5.05$, $c = 8.28$A. Photographs of the 0*kl* net of the OC phase at 370°C and of the corresponding *hkl* [$h = 1/2(h_{OC} - k_{OC})$, $K = k_{OC}$, and $l = l_{OC}$] net of the HP phase at 380°C are shown in Figures 8a and 8b. The photograph at 380°C indicates that reflections of the type *hkil* with $l \neq 2n$ (if $h - k = 3n$) are present, but extremely diffuse and weak compared with the corresponding reflections of the OC phase. This extra extinction is related to the following atomic coordinates. The locations of all atoms in the HP phase can be expressed by special positions, *i.e.*, six oxygen atoms are in 6(g), two oxygen atoms in 2(c), and four silicon atoms in 4(f) in space group $P6_3/mmc$. This structure is identical with the proposed structure of Gibbs (1927).

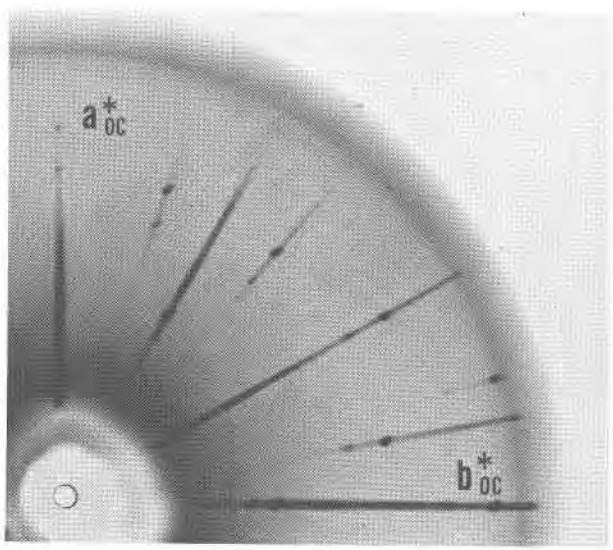

Fig. 6. Photograph of the *hk*0 net of the OC phase at 260°C.

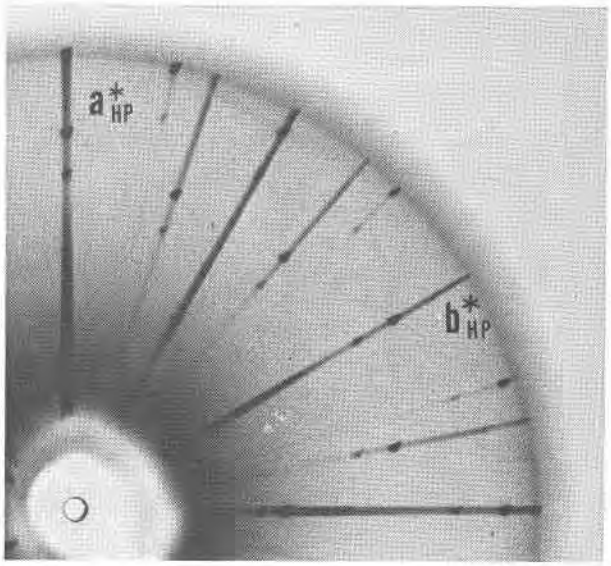

Fig. 7. Photograph of the *hk*0 net of the HP phase at 380°C.

On the other hand, Figure 1h reveals that the OC and HP phases coexist under the given experimental conditions. By X-rays, at the vicinity of 380°C reflections *hkil* with $l \neq 2n$ still remain, weakly. These reflections become extremely weak and gradually fade into background with increasing temperature up to 450°C. Therefore, at higher temperatures, the HP phase will be identical with the ideal hexagonal structure, where tetrahedra are arranged as layers with their bases perfectly parallel to $(001)_{HP}$.

Discussion

Thermal changes of tridymite described previously by other authors are schematically shown in Figure 9.

Most of them were determined by differential thermal analysis (DTA) or X-ray powder diffraction. However, the reported transition temperatures differ from each other. The first transition seems to be in the range between 105° and 120°C, the second between 150° and 175°C, and the last between 440° and 475°C. According to Sosman (1965), the differences in transition temperature have been considered to be due to various experimental conditions such as intimate mixtures, twinning, impurities, and so on. Furthermore, Sosman indicated that the first and second transitions are common to both types of tridymites S and M, and those at 64°, 210°, and 475° are not critical because there are no abrupt changes of heat effects at those temperatures.

In the present study, phase boundaries were observed at 110°, 150°, 190°, and 380° up to 450°C. These transitions are also confirmed in the changes of the optical microscopic figures. The transition temperatures are determined by the beginning of gradual changes. The transitions from MC to OP phases and from OP to OS phases show critical changes under X-ray and optical observations. However, transition from OS to OC phases is difficult to detect by X-ray, since the change from the satellite reflections to diffuse streaks is not clear. However, optical observation indicates a critical change showing a rapid formation of domains in a narrow temperature range at the beginning of the transition. In contrast, the beginning and end of the transition from the OC to HP phases are not clear under the microscope but are critically sharp in X-ray diffraction patterns. The transition temperatures presently observed are thus rather accurate, since the X-ray single-crystal method was used in parallel with the optical method.

Some differences are present between the present results and the data summarized by Sosman. First, the transition at 64°C was not detected in the present study by X-ray and optical methods. The transition at 64°C was previously observed as 2θ peak changes in X-ray powder diffraction patterns (Hill and Roy, 1958). Sato (1964) observed the transition at 64°C in more detail by X-ray powder diffraction, using a specimen with unit cell $a = 10.04$, $b = 17.28$, $c = 8.20$A, and $\beta = 91.50°$. This transition was explained by the slight change of β angle between the S1 and S2 phases. However, this transition has not been found by DTA up to the present.

On the other hand, the transition at 380°C found in the present study has not been reported previously. The transition at 380°C is substantial; it is the first-order change from orthorhombic to hexagonal. With regard to the presence of the transitions at 64° and 380°C, the causes of the discrepancies between different studies are not clear. However, the possibility cannot be neglected that these discrepancies may be due to some unspecified differences in the nature of the starting materials.

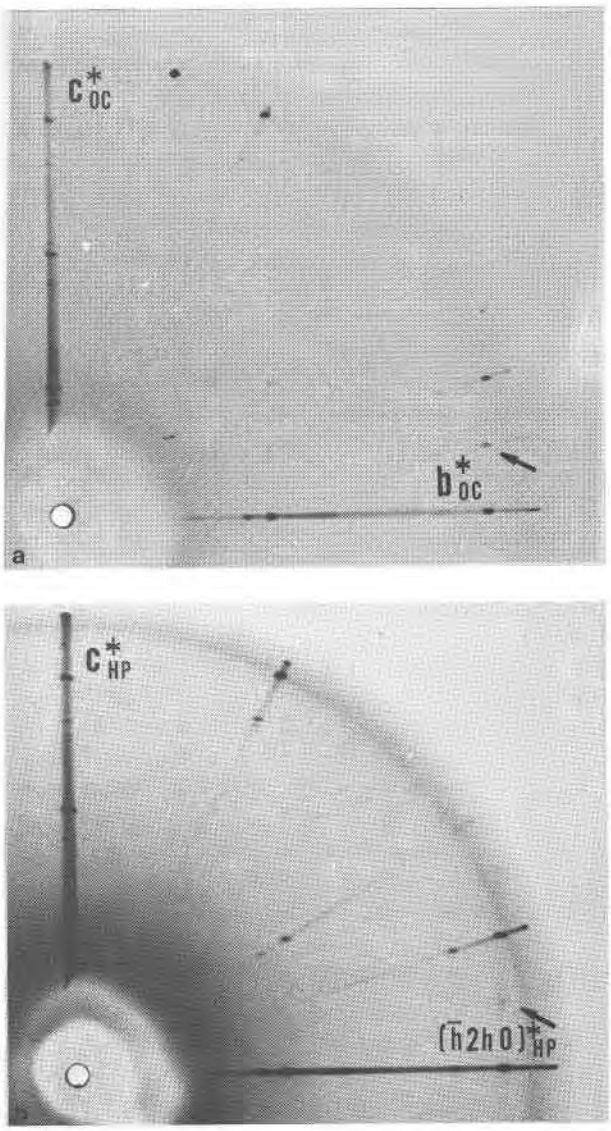

Fig. 8. Precession photographs of the $0kl$ net of the OC phase at 370°C (a) and of the corresponding $hkil$ [$h = 1/2(h_{OC} - k_{OC})$, $k = k_{OC}$ and $l = l_{OC}$] net of the HP phase at 380°C (b).

From the structural point of view, the transitions observed are consistent with the tendency of higher-temperature modifications to have higher symmetry. This tendency is also confirmed in the atomic arrangements. In the "ideal" hexagonal structure, the Si–O–Si bond angles are exactly 180° in space group

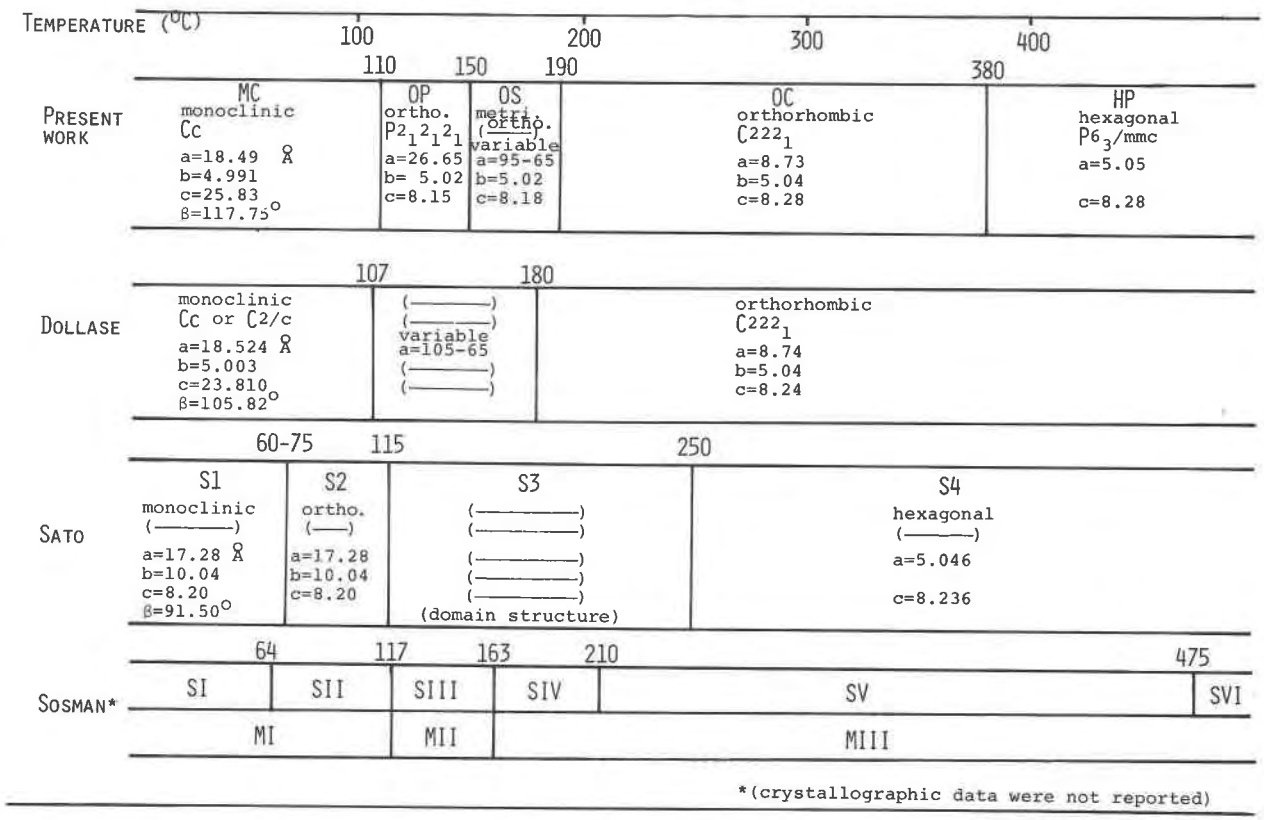

Fig. 9. Thermal changes of tridymite and crystallographic data of each phase stable below about 500°C. Symbols of the phase symmetry, space group, and cell edges are listed in the column, and the transition temperature is at the head of the column.

P6₃/mmc. In the OC phase, the Si–O–Si bond angles normal to the silica layer are 178.2° and those in the layer 171.2° and 165.2° (Dollase, 1968). On the other hand, in the MC phase the Si–O–Si bond angles normal to the silica layer are in the range from 143.8° to 156.7°, except for an extremely large angle of 176.4°, and those in the layer range from 143.2° to 155.7° (Kato and Nukui, 1976). The Si–O–Si bond angles of lower-temperature modifications tend to settle down to some intermediate value of the Si–O–Si bond angles between the OC and MC phases.

The satellite reflections observed in the a^*_{OS} direction of the OS phase above 150°C are quite interesting from this Si–O–Si bond angle point of view, because of their non-integral nature. The satellite reflections may be mainly influenced by the lattice modulation "wavy shift" of the atomic positions, because the intensities of satellite reflections at higher indices are stronger than those at lower indices. The wave of the shifts of atomic positions is considered to be due to the wavy change of the Si–O–Si bond angles along $[100]_{OS}$ ($[210]_{HP}$) in the OS phase. The average bond angle of the Si–O–Si bond may therefore be some intermediate value of those of the MC and HP phases. With increasing temperature, the spacing of satellite reflections (OS phase) becomes longer, and conversely the wave length of lattice modulation is shortened. The relative intensities of the higher-order satellite reflections compared with the first-order reflections are weakened at higher temperatures and disappear near the transition (from OS to OC phases) temperature. The modulation wave is thus randomized, and satellite reflections change to diffuse streaks at the transition. On the other hand, with decreasing temperature, modulation wave length becomes longer, and at last satellite reflections change into reflections of the OP phase. This tendency is quite interesting when compared with other non-integral superstructures. A detailed study on the non-integral nature of tridymite will be the subject of a future discussion.

Acknowledgments

The authors thank Dr. K. Hirota of this Institute who kindly supplied the present crystals, and Dr. M. Watanabe for utilization of the furnace for the precession camera. We express our gratitude

to Dr. T. Shimohira and Professor S. Iwai for their interest in the present work.

References

Buerger, M. J. and J. Lukesh (1942) The tridymite problem. *Science, 95,* 20–21.

Dollase, W. A. (1968) The crystal structure at 220°C of orthorhombic high tridymite from the Steinbach meteorite. *Acta Crystallogr., 23,* 617–623.

——— and W. H. Baur (1976) The superstructure of meteoritic tridymite solved by computer simulation. *Am. Mineral., 61,* 971–978.

Fenner, C. N. (1913) The stability relations of the silica minerals. *Am. J. Sci., 36,* 331–384.

Gibbs, R. E. (1927) The polymorphism of silicon dioxide and structure of tridymite. *Proc. Roy. Soc. (Lond.), A113,* 361–368.

Götz, W. (1962) Untersuchungen am Tridymit des Siderophyrs von Grimma in Sachen. *Chem. Erde, 22,* 167–174.

Hill, V. G. and R. Roy (1958) Silica structure studies VI. On tridymites. *Trans. Brit. Ceram. Soc., 57,* 496–510.

Kitamura, M. and N. Morimoto (1975) The superstructure of intermediate plagioclase. *Proc. Japan Acad., 51,* 419–424.

Kato, K. and A. Nukui (1976) Die Kristallstructur des monoklinen Tief-Tridymits. *Acta Crystallogr., B32,* 2486–2391.

Konnert, J. H. and D. E. Appleman (1975) Terrestrial low tridymite: refinement of the three-dimensional structure (abstr.). *Geol. Soc. Am. Abstracts with Programs, 7,* 1151.

Megaw, H. D. (1960) Order and disorder III. The structure of the intermediate plagioclase feldspars. *Proc. Roy. Soc. (Lond.), A259,* 184–202.

Nakazawa, H. and N. Morimoto (1971) Phase relations and superstructure of pyrrhotite, $Fe_{1-x}S$*. *Mater. Res. Bull., 6,* 345–358.

Sato, M. (1964) X-ray study of tridymite (3) unit cell dimensions and phase transition of tridymite, type S. *Mineral. J., 4,* 215–225.

Sosman, R. B. (1965) *The Phases of Silica.* Rutgers University Press, New Jersey.

Manuscript received, August 19, 1977; accepted for publication, February 18, 1978.